Optimization of microchip-based capillary electrophoresis for studying oncolytic adenovirus-peptide binding ratio

Batelić, Laura

Laura Batelić

Optimization of microchip-based capillary electrophoresis for studying oncolytic adenovirus-peptide binding ratio

DIPLOMA THESIS

Submitted to The University of Zagreb, Faculty of Pharmacy and Biochemistry

In Zagreb, 2019

Contents

List of Abbreviations

CE	capillary electrophoresis
EOF	electroosmotic flow
FITC	fluorescein isothiocyanate
LIF	laser-induced fluorescence
LOD	limit of detection
LOQ	limit of quantitation
MCE	microchip capillary electrophoresis
MHC-I	major histocompatibility complex class I
OSTE	off-stoichiometric thiol-ene
PDMS	polydimethylsiloxane
PEG	polyethylene glycol
PEPTICRAD	peptide-coated Conditionally Replicating Adenovirus
R_{110}	rhodamine 110 chloride
RSD	relative standard deviation
SD	standard deviation

1 Introduction

1.1 Microchip Electrophoresis

Efficient separation of drugs from their impurities or biotransformation products is one of the most essential tasks of drug discovery and development. Microfluidic separation devices have been shown to provide significant improvement in terms of analytical throughput by enabling separation times in the range of one minute. Microchip capillary electrophoresis is currently the gold standard for microfluidic separation. Capillary electrophoresis (CE) in its different modes of operation is demonstrated to be a separation technique suitable to be integrated into a planar microdevice. CE proved to be an excellent match for microchip technologies because it easily manipulates volumes at the nanoliter scale, requires no moving parts, and provides fast, high-resolution separations (Manz et al., 1992). The process of miniaturization of CE to the microchip is facilitated by its relatively simple technical arrangement and by the high efficiency of electrophoretic separations. The main objective of these efforts is to develop so-called micro-total analysis systems (μ-TAS) which will integrate different steps of analytical process into one miniaturized flow system enabling much faster, fully automated analysis (Manz et al., 1990). Microchip electrophoresis possesses several advantages above CE such as a significant reduction of analysis time, a lower cost due to the reduction of consumption of sample and reagents and on-line coupling of various processes to a single device (Ramsey et al., 1995). Unlike traditional CE instrumentation, which consists of essentially a single capillary (or an array of capillaries in parallel), many different capillaries and fluidic channels can be patterned on a microfluidic device, providing the potential for high-throughput, massively parallel analysis.

The first microchip CE systems were constructed using glass as a material (Jacobson et al., 1994; Manz et al., 1992). Glass, being a silica compound, has well-known and well-developed microfabrication methods that were adapted directly from the semiconductor engineering field. Despite excellent optical properties and same surface chemistry as the fused silica capillaries in conventional CE, glass microchips have many disadvantages. First, the fabrication process yields one device, resulting in a relatively high manufacturing cost per microchip. Second, glass is fragile and easily broken if not handled with extreme care. Third, high quality glass is expensive. As a result of these issues, a significant amount of attention has focused on the fabrication of microchips using polymer substrates.

Polymer substrates are less expensive and easier to fabricate than glass. Polymers can be fabricated for example by a molding procedure or by the use of direct writing protocols using ultraviolet lasers, electron beams, or X-rays. Both fabrication methods provide high-throughput and use lower cost materials. The major limitation of polymers for microchip CE is the poorly understood and poorly controlled surface chemistry of these materials. Understanding and controlling the material properties of polymer devices is an important goal. Among all the polymers, PDMS is certainly the most common due to its elastomeric properties, optical transparency, biocompatibility and low cost, making this a very good substrate for method development (McDonald and Whitesides, 2002). However, PDMS has an extremely hydrophobic surface that makes PDMS prone to unwanted, nonspecific adsorption of proteins (Wang et al., 2009) and small molecules (Gomez-Sjoberg et al., 2010). Moreover, PDMS devices generate unstable electroosmotic flow and this can affect the electrophoretic separation efficiency on these devices (Vickers et al., 2006). All of this information lead to necessity for fabrication of new polymer materials with better properties.

1.2 Microchannel Surface Coatings

In classical electrophoresis it is well known that the reproducibility and the performance of separations can be improved by appropriate surface modification. Internal capillary coatings are applied to control electroosmotic flow and to suppress analyte-wall interactions. That said, surface chemistry is of great importance in miniaturized and integrated systems due to high surface area-to-volume ratio. Belder *et al.* gave some additional aspects why surface chemistry appears to be even more important in MCE:

1) Control of electroosmotic flow (EOF). Common injection processes like pinched and gated injections rely on a reproducible electroosmotic flow. Stabilization of EOF is important in order to improve the precision of migration times. The stability of flow in repetitive runs is often unsatisfactory because of the adsorption of sample and buffer components at the surface which alters the ζ-potentials and by that EOF. In order to recondition the surfaces of microfluidic chips and to stabilize EOF, excessive rinsing and etching steps are often applied. In addition, nonuniform surface properties can lead to different EOF velocities, especially in intersected channels which leads to pressure gradients and hydraulic pumping

(Culbertson et al., 2000; Herr et al., 2000). In that case, a parabolic flow profile is observed which leads to band broadening.

2) Reduction of analyte-wall interaction. Appropriate surface coatings lead to reduction of analyte-wall interactions which increases separation efficiency and by that resolution. The obtainable resolution in MCE is in practice often lower than in classical CE due to the limited separation channel length. Accordingly, the optimization of resolution is of great importance.

Coatings can be separated in two categories: permanent and dynamic coatings (physical adsorbed coatings). In permanent coatings chemical compounds (often polymers) are covalently bound to functional groups of the surface or immobilized (via cross-linking of a polymer) at the surface to become insoluble in the electrolyte. For dynamic coating dissolved surface-active compounds are utilized which adsorb strongly at the surface. This can be done by rinsing with a solution of the modifier before analyses or by addition of the modifier to the electrolyte.

Although dynamic surface modification is very convenient and popular there are some unfavorable sides to it. A drawback is the limited stability that makes it crucial either to add the compound to the running electrolyte or to repeatedly regenerate the coating by rinsing step. The presence of surface-active compound in the electrolyte can influence the electrophoretic separation and interfere with detection (Belder and Ludwig, 2003).

1.2.1 PEG Coating

Protein and other biomolecules adsorption on solid surfaces is a complex phenomenon and appears to involve many dynamic steps such as bond formation between proteins and surfaces, lateral diffusion on the surface and conformational changes and rearrangements of adsorbed proteins. Main reasons for protein adsorption are hydrophobic interactions, electrostatic attraction, van der Waals and hydrogen bonding (Roach et al., 2005). Elimination of protein adsorption requires the suppression of all of these attractive forces between proteins and surface. In this research Polyethylene glycol (PEG) was used for covalent modification of microchannel surfaces. PEG coating is important in protein separations, which are challenging in uncoated devices due to their strong adsorption to the channel surface. PEG molecules attached to the surfaces have shown high potential as a protein repellent due to

their flexibility and high water solubility (Archambault and Brash, 2004; Kingshott et al., 2003; Wei et al., 2003; Zhang et al., 2001). In addition to being hydrophilic, PEG is non-toxic and offers exceptional biocompatibility, making it an ideal material for biological applications. It has been suggested that PEG chain length, conformation and number density on the surface are important factors for resisting protein adsorption (Archambault and Brash, 2004; Roosjen et al., 2004; Unsworth et al., 2005; Wei et al., 2003). That said, surfaces forming a big number of hydrogen bonds with water molecules produce large repulsive forces on the protein, leading to lower protein adsorption (Zheng et al., 2005). On the other hand, there is also evidence that indicates in some cases PEG binding to proteins (Efremova et al., 2001; Sheth and Leckband, 1997).

1.3 Polymer Microchips

Today, there is a substantial number of different polymers that have been used for the fabrication of microfluidic devices instead of glass and silicon. Plenty of them are in regular use and commercially available. The material choice is based namely on the material properties as well as the ease of mass production (Becker and Gärtner, 2008). The latter is an analytical issue because it affects not only the cost but also the reproducibility of chip-based analyses. The material properties such as chemical stability and surface chemistry are probably the most important aspects since they greatly define the applications in which the particular material can, or cannot, be used (Volpatti and Yetisen, 2014).

Thiol-ene polymers represent UV-curable systems that have all the requirements for a microfluidic rapid prototyping (Carlborg et al., 2011; Natali et al., 2008; Sikanen et al., 2013). Properties of polymerization of thiol-enes which are good for chip fabrication are delayed gelation point, low volume shrinkage stress, uniform network formation even without initiators and low oxygen inhibition (Cramer et al., 2004, 2002). Very low polymerization shrinkage stress allows thin device sections without warpage, the rapid reaction leads to manufacturing device in the order of seconds and the availability of different multifunctional monomers allows for a large variety of mechanical and chemical properties. The specificity of the reaction and the unique alternating step-growth mechanism lead to well-defined homogeneous polymer networks that have very useful material properties such as excellent optical clarity, a narrow glass transition and low permeability to common solvents (Cygan et

al., 2005; Natali et al., 2008). Thiol-ene reaction belongs to a family of so called "Click" reactions that imply a set of a powerful, very specific, and highly reliable "lock and key" reactions (Cramer and Bowman, 2001; Hoyle and Bowman, 2010). Thiol-ene photopolymerizations are step-growth radical photopolymerizations based on the addition of a thiol (-SH) to a monomer with an ene-functional group (carbon double bond). Normally, the reaction is triggered with a photoinitiator but it can also be triggered spontaneously with low wavelength UV-irradiation (Cramer et al., 2002).
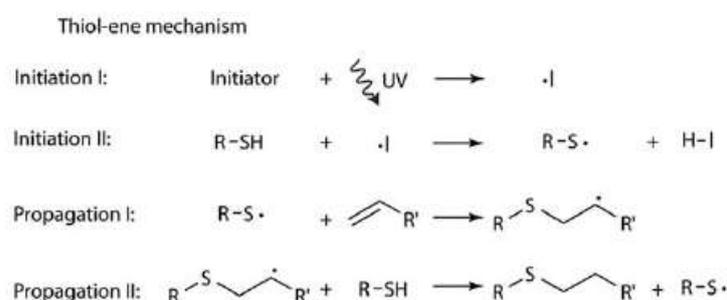

Figure 1. Reaction mechanism of UV-initiated radical thiol-ene coupling (Carlborg et al., 2011).

The radical removes a hydrogen atom from the thiol to form a thiyl radical (Initiation II) and the reaction propagates by a rapid cascade of polymerization reactions that in short time convert the liquid prepolymer into a solid polymeric material (Figure 1). First, the thiyl radical is added to an ene-functional monomer (Propagation I) and after that a chain transfer of the radical to a thiol functional group takes place, regenerating a thiyl radical (Propagation II). The chain step is responsible for the final properties of the polymer since it imparts delayed gelation and a high ultimate conversion, thanks to decreased tendency of radicals to become trapped in the forming polymer network. It is well known that polymerization reactions reduce the monomer distance so any reactions happening after the transformation from a liquid to a solid (the gel point) lead to shrinkage stress. Delayed gelation of thiol-enes greatly reduces the shrinkage stress experienced in the final material compared with other commonly used thermoset materials where the gel point is reached early on in the polymerization (Lu et al., 2004). There are two reasons for homogenous network; firstly, the

almost perfectly alternating reaction mechanism between thiols and enes that are sufficiently electronegative to prevent homopolymerization; and secondly the high conversion possible in most thiol-ene polymerizations reduce the presence of regions with a low crosslink density since almost all reactive groups are tied into network. Because of that, irregular features such as chain ends and regions with significantly higher crosslink densities are largely avoided (Carlborg et al., 2011).

Standard stoichiometric formulations of thiol-ene systems lead to a complete polymerization and the absence of functional groups on the surface and in the bulk (Figure 2). Stoichiometric thiol-ene polymer is made of two types of monomer. One with thiol functional groups, xR_1-$(SH)_m$, and the other with allyl functional groups, yR_2-$(CH_2$-CH=$CH_2)_n$, where y and x are the number of monomers of each type and n and m are the number of functional groups on each. Thiol-ene systems normally strive to maximal mechanical strength and in order to achieve that there has to be exact equal number of monomers of each type of functional groups, yn=xm, with very few or no reactive groups remaining.
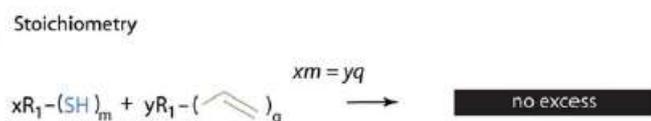

Figure 2. Standard stoichiometric formulation of thiol-ene polymer without reactive functional groups (Carlborg et al., 2011).

The novel off-stoichiometry thiol-ene formulations provide mechanical properties controlled by tuning the monomer mixing ratios, where properties range from PDMS-like elastomeric properties to thermoplastic stiffness. Carlborg *et al.* proposed the use of off-stoichiometric thiol-ene (OSTE) polymers as substrates for microfluidics. These substrates are fabricated by mixing thiol and ene precursors in a non-stochiometric ratio (Figure 3). By adding an excess of one of the two precursors it is possible to obtain a final polymer with surface properties matching those of the excess reagent used. The most rigid polymer layers are obtained by using the stoichiometric composition or an excess of allyls and as a result these polymers can resist the highest pressures. On the other hand, the excess of thiol monomers produce more elastic polymers and thus decrease the pressure tolerance. By using monomers with more thiol groups (e.g. tetrathiol versus trithiol), a higher cross-linking ratio, and thus, greater stiffness is obtained (Sikanen et al., 2013).
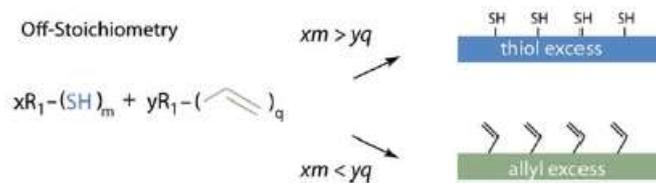
Figure 3. Off-stoichiometric formulation of thiol-ene polymer with reactive functional groups (Carlborg et al., 2011).

As advantages, the curing time can vary from 30 to 180 s, which is much faster than curing time of the commonly used PDMS. Also, the presence of readily available functional groups on the surface of OSTE substrates is beneficial for surface modifications and bonding.

1.4 Peptide-coated Conditionally Replicating Adenovirus (PeptiCRAd)

In this research the goal was to develop MCE-LIF method for studying oncolytic adenovirus-peptide binding ratio. Capasso *et al.* suggested a novel oncolytic vaccine platform (PeptiCRAd) in which tumor peptides are not expressed by the virus and are not part of the viral proteins, in contrast to the vast majority of the current approaches. The peptides are instead adsorbed onto the viral capsid, allowing for the efficient co-delivery of adjuvant (virus) and tumor-specific epitopes. Thus, the oncolytic virus acts as an "active" carrier that is able to kill tumor cells and to boost the immunological response against the chosen antigen. This method does not involve chemical or genetic modification of the virus, significantly increasing the rapidity and the versatility of the preparation. As a direct consequence, this system addresses the need for tumor-specific and even personalized therapies that could account for the expression of different antigens in different patients or different antigens in different stages of the same tumor. By absorbing tumor-specific MHC-I-restricted peptides onto the viral capsid, the immunity can be directed toward the tumor, leading to a significantly increased efficacy. Since the adenovirus capsid is negatively charged (Fasbender et al., 1997) the hypothesize is that MHC-I-restricted peptides, modified to become positively charged, would bind to the capsid of the virus via electrostatic interactions (Capasso et al., 2015).

2 Aim

The aim of this thesis was to develop microchip-based capillary zone electrophoresis method for studying oncolytic CpG adenovirus-peptide binding ratios by MCE-LIF. Since the PeptiCRAd vaccine is a new cancer platform, it would be interesting to know more details about specific binding ratios between tumor-specific MHC-1 restricted peptides and viral capsid and this can be done by MCE because the analytes are charged. To develop the MCE method, first the detector settings were optimized by fluorescein. Fluorescein was taken as a model analyte because the peptides used in research have been fluorescently labeled with fluorescein isothiocyanate (FITC-peptides). Optimization of MCE-LIF method was done with fluorescein and FITC-SIINFEKL peptide (non interactive with virus) as analytes. Even though MCE is a convenient method for rapid determination of virus-peptide interactions, it is challenged by the strong nonspecific surface adsorption of the multiply charged peptide. To overcome analyte adsorption two different surface modifications were tested: covalent PEGylation on allyl-rich thiol-ene microchannel surfaces and the new dynamic non-labeled peptide coating on thiol-rich thiol-ene microchannel surfaces.

3 Materials and Methods

3.1 Chemicals

All chemicals used in this work are listed in Table 1.

Table 1. List of chemicals with suppliers and control numbers used in research.

Chemicals	Supplier	CAS
PolyK-SIINFEKL peptide (M_w 2195 Da) = FITC-6K-peptide	Zhejiang Ontores Biotechnologies Co., Zhejiang, China	n/a
SIINFEKL peptide (M_w 1295 Da) = FITC-peptide	Zhejiang Ontores Biotechnologies Co., Zhejiang, China	n/a
PolyK-SIINFKEL peptide (non fluorescent, dynamic coating)	Zhejiang Ontores Biotechnologies Co., Zhejiang, China	n/a
Monofunctional Poly(ethylene glycol) (PEG) Sulfhydryl, (mPEG-SH) , MW=1000	Creative PEGWorks, Chapel Hill, NC, USA	25322-68-3
1,3,5-Triallyl-1,3,5-triazine-2,4,6(1H,3H,5H)-trione	Sigma Aldrich Co., Steinheim, Germany	1025-15-6
Pentaerythritol tetrakis(3-mercaptopropionate)	Sigma Aldrich Co., Steinheim, Germany	7575-23-7
Trimethylolpropane tris(3-mercaptopropionate)	Sigma Aldrich Co., Steinheim, Germany	33007-83-9
SYLGARD® 184 Silicone elastomer curing agent and base	The Dow Chemical Company, Midland MI, USA	n/a
Sodium hydroxide	Merck, Darmstadt, Germany	1310-73-2
Dimethyl sulfoxide (DMSO)	Sigma Aldrich Co., Steinheim, Germany	67-68-5

Sodium phosphate dibasic dihydrate	Sigma Aldrich Co., Steinheim, Germany	10028-24-7
Sodium phosphate monobasic dihydrate	Sigma Aldrich Co., Steinheim, Germany	13472-35-0
MQ water, deionized	Mili-Q water purification system	-
Fluorescein	Sigma Aldrich Co., Steinheim, Germany	2321-07-5
Rhodamine 110 chloride	Sigma Aldrich Co., Steinheim, Germany	13558-31-1
Boric acid	Riedel-de Haën, Seelze, Germany	10043-35-3

3.1 Microchip Thiol-ene Fabrication

The chip fabrication process (Figure 4) includes four steps: (a) SU-8 master fabrication in the cleanroom, (b) casting of a PDMS mold with the help of the SU-8 master (non-cleanroom), (c) fabrication of thiol-ene microchannel and cover layers using PDMS mold, and (d) bonding of the thiol-ene layers.
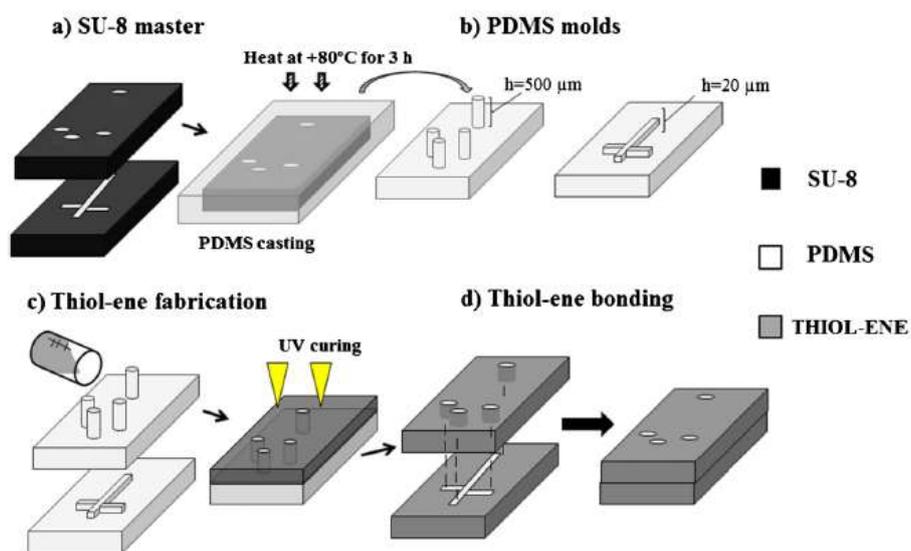

Figure 4. Schematic view of the fabrication of a thiol-ene microchip (Tähkä et al., 2015).

SU-8 masters and PDMS molds were fabricated individually for both cover (inlets) and microchannel layers and could be reused for replication several times. PDMS molds were made by using elastomer base (Sylgard 184 Slicone Elastomer Base, Dow Corning) and curing agent (Sylgard 184 Slicone Elastomer Curing Agent, Dow Corning) at the ratio of 10 to 1. After mixing, the mixture was filled with air bubbles so it was placed in the vacuum desiccator to remove them. Once properly stirred and excess air removed, SU-8 master (inlet master or microchannel master) was placed on a plastic Petri dish and the PDMS mixture was then poured on top of the plate. Air bubbles generated when pouring the mixture were removed with the plastic stirrer. The Petri dish with SU-8 master and PDMS mixture on top of it was then put in the oven at 70-90°C for three hours in order to polymerize PDMS. Petri dish was removed from the oven after the monomer mixture was cured. The PDMS mold had to be detached from the SU-8 master carefully to avoid damaging the microchannels.

The thiol-ene chips were made from commercially available monomers by mixing either trithiol with triallyl or tetrathiol with triallyl in varying ratios. The thiol-rich thiol-ene microchips with 50% excess of thiol functional groups were made by using Pentaerythritol tetrakis(3-mercaptopropionate) (tetrathiol monomer) and 1,3,5-Triallyl-1,3,5-triazine-2,4,6($1H,3H,5H$)-trione (triallyl monomer). The allyl-rich thiol-ene microchips with 50% excess of ene functional groups were made by using Trimethylolpropane tris(3-mercaptopropionate) (trithiol monomer) and 1,3,5-Triallyl-1,3,5-triazine-2,4,6($1H,3H,5H$)-trione (triallyl monomer). Photoinitiator wasn't used during the thiol-ene fabrication process. After mixing, the monomer solution was poured onto the PDMS mold (inlet/cover mold) and cured for 10 minutes by using a Dymax 5000-EC Series UV flood exposure lamp (Dymax Corporation, Torrington, CT, USA, nominal power of 225 mW/cm^2). Next, another thiol-ene layer was cured in the same manner in the PDMS mold (microchannel mold). The inlets on thiol-ene cover layer were drilled (Ø1.5 mm) before the bonding step. The drilling dust was carefully cleaned before bonding by drying with nitrogen gas. After that, both layers (inlet and microchannel layer) were put in the oven for a brief (1 minute) to soften before attaching them one to another. When attached, the chip was immediately placed again under UV lamp to cure the wafers. The last exposure to UV light was 5 minutes long after which the chip was allowed to cool down to room temperature. When the chip was cooled down Zeiss microscope was used to check the integrity of the microchannels.

3.2. Sample Preparation

All buffers were prepared in deionized Milli-Q water (Millipore, Bedford, MA) to yield a final ion concentration of 20 mM and adjusted to the desired pH by pH meter. Sodium phosphate buffer (pH 7,40) was prepared by using monobasic sodium phosphate and dibasic sodium phosphate which were purchased from Sigma-Aldrich (Steinheim, Germany). Sodium borate buffer (pH 10,00) was prepared by using boric acid and sodium hydroxide. The stock solutions of fluorescein were prepared in dimethyl sulfoxide (5,00 mM), after which they were diluted with 20 mM sodium borate buffer (pH 10,00) to obtain concentrations of 1,25 nM -1 µM. The sample solutions of FITC-SIINFEKL peptide (1,25 g/L in H_2O) were diluted with 20 mM sodium phosphate buffer (pH 7,40) to obtain concentrations of 0,5-100 mg/L. The stock solutions of rhodamine 110 chloride were prepared in dimethyl sulfoxide (5,00 mM), after which they were diluted with 20 mM sodium phosphate buffer (pH 7,40) to get concentrations of 100 nM and 300 nM.

3.3. Microchip Capillary Electrophoresis

Standard electrophoresis chip designs featuring separation channel of 55-85 mm and simple cross injectors were used (Figure 5). The effective separation length was 40 mm in all MCE-LIF analyses. All thiol-ene microchannels were sequentially rinsed with deionized Milli-Q water and the separation buffer with negative (vacuum) pressure applied for 2-5 minutes. The choice of buffer was determined by the sample that was used in measurements. For fluorescein samples the sodium borate buffer (pH 10,00) was used and for the rhodamine and FITC-SIINFEKL peptide samples the sodium phosphate buffer was applied (pH 7,40). Before analysis, the microchannels inlets were filled with fresh buffer solution and 10 µL of the buffer was applied to the buffer inlet, buffer waste and sample waste reservoirs. Sample (8 µL) was applied to the sample inlet right before the beginning of measurements. The buffer and sample volumes were adjusted in order to induce minor hydrodynamic flow of the fresh buffer toward the injection channel inlet and outlet, and thus prevent sample leakage to the separation channel, prior to injection, whereas the electric field during injection was adjusted to overcome hydrodynamic flow by electrokinetic flow (Figure 5.). The MCE analysis was performed in 20 mM sodium borate buffer (pH 10,00) or sodium phosphate buffer (pH 7,40) (depending on the choice of sample) at 500 Vcm^{-1}. In order to prevent sample leakage, small

push-back voltages were applied to the sample inlet and sample outlet during separation (Figure 5.).
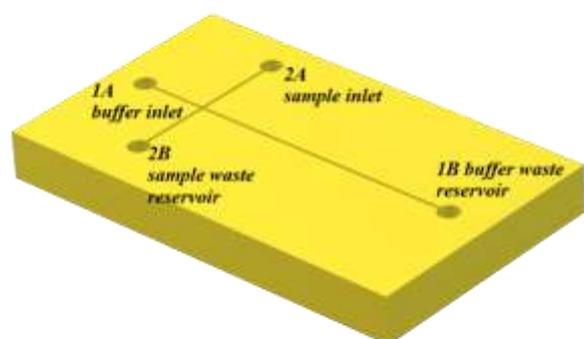
Steps	Duration of steps	Applied Voltages per each inlet			
		1A/kV	1B/kV	2A/kV	2B/kV
Injection step	25 s	0,6	flt	0,8	gnd
Floating step	1 s	flt	flt	flt	flt
Separation step	79 s	3,06	gnd	2,5	2,5

Figure 5. Microchannel design for MCE: An injection cross design features a sample channel (2A-2B) that crosses the separation channel (1A-1B). In order to prevent sample leakage, small push-back voltages were applied to the sample inlet and sample outlet during separation. Electric field during injection was adjusted to overcome the hydrodynamic flow by electrokinetic flow.

3.4. Instrumentation

A computer-controlled (Labview) high voltage power supply (Microfluidic Tool Kit, Micralyne, Edmonton, Canada) was used to obtain the separation voltages and to record current readings. Laser-induced fluorescence detection was accomplished with two different epifluorescence microscope. One was Leica DMIL inverted epifluorescence microscope (Leica Nilomark, Espoo, Finland) equipped with an N PLAN L20 x /0,40 corr. objective and a JDSU FCD488 (488 nm; 20 mW) continuous wave solid state laser (Cheos Oy, Espoo, Finland). The other one was Zeiss Axioscope A1 upright epifluorescence microscope (Carl Zeiss Oy, Espoo, Finland) equipped with a Plan Neofluar 10x/0,30 objective and a continuous wave argon laser (488 nm, nominal power 75 mW, JDS Uniphase, Cheos Oy, Espoo,

Finland). The fluorescence emission (500-700 nm) in both microscopes was collected perpendicular to the microchip, through a detection slit, to a Hamamatsu R5929 photomultiplier tube equipped with integrated housing and a signal amplifier module (Cairn Research, Faversham, UK). Photomultiplier tube settings used in this research are listed in the Table 2. A PicoScope 2203 AD converter and PicoLog software (Pico Technology, St. Neots, UK) were used for recording the signal. The analysis peaks were analyzed and integrated with CSW32 Chromatography Station Software. Statistical data analysis was achieved by using the Regression tool included with Analysis ToolPak in Microsoft Excel.

Table 2: Photomultiplier settings used:

Photomultiplier settings:	
Average bandwidth	10 Hz
Integrator gain	M
Integrator time	50 ms
PMT volts	900 V
PMT gain	H (5) (Zeiss microscope)
PMT offset	H
Average/Integrate	Integrate

3.5. Microchip Channel Surface Modification

In the work non-coated microchips (native) and coated microchips were used. Native microchips with 50% molar excess of tetrathiol monomer (Thiol-rich thiol-ene chips) and native microchips with 50% molar excess of triallyl monomer (Allyl-rich thiol-ene chips) were used in tests. On allyl-rich thiol-ene chips traditional PEGylation (methoxy-PEG-thiol MW 1000) was used on the channels (Figure 6). A concentration of 2 mg/mL of polyethylene glycol (in methanol/water 80:20, v/v) was introduced into the capillary and cured by UV for 1 minute. That procedure was repeated three times. Before use, channels were rinsed with the running buffer for 2 minutes. Thiol-rich thiol-ene channels were modified with 1g/L solution of polyK-SIINFEKL, non labeled 6K-peptide (Figure 6). The channel surface was pretreated by 0,1 M sodium hydroxide (for 2 minutes) and deionized water (for 5 minutes). After filling the thiol-rich chip with non labeled 6K-peptide, the chip was left to stabilize for 15 or 30

minutes. Before measurements, both of the modified channels were rinsed with the running buffer for 2 minutes. Rhodamine 110 chloride was tested prior to FITC-SIINFEKL and PolyK-SIINFEKL peptides to be sure that the microchannels are successfully coated with polyethylene glycol and peptide analogue. The success of the coating onto the surface was based on comparison of the migration time of Rhodamine 110 chloride peaks in native and coated microchannels.
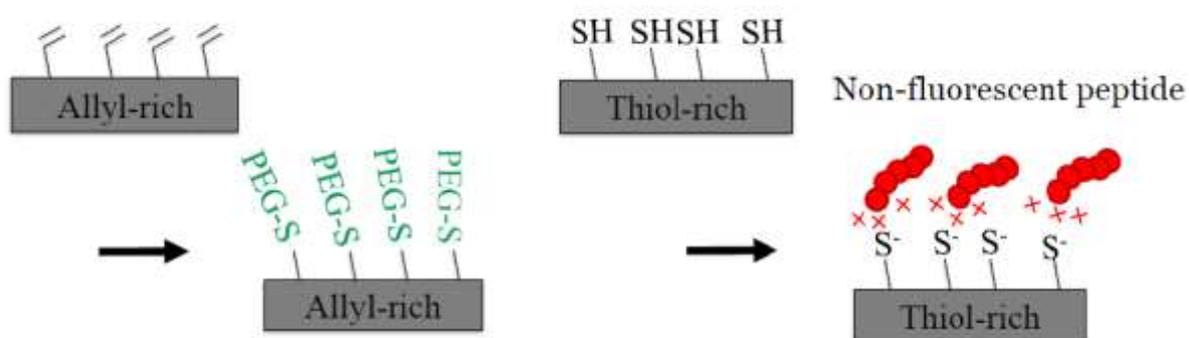

Figure 6. Covalent PEGylation of allyl-rich surfaces and dynamic coating of thiol-rich surfaces with peptide analogue.

4. Results and discussion

In this work, the aim was to study positive peptide binding on negatively charged viruses by microchip electrophoresis. First, the detector and separation conditions were optimized by fluorescein. Under optimized detector conditions LOD/LOQ values and linearities were determined for fluorescein and the FITC-SIINFEKL peptide. Fluorescein was chosen as a model analyte because peptides used in research were fluorescently labeled with fluorescein isothiocyanate (FITC-peptides) and the method of detection was laser-induced fluorescence. Preliminary results of two tested surface modification are presented in the Chapter 4.7.

4.1. Optimization of Detection Window Size

For the determination of the size of detection slit, 1 µM fluorescein was used and studied by MCE-LIF on allyl-rich thiol-ene microchip. Two different sizes of detection window were tested. A detection window of 50 µm x 200 µm (1:4 ratio) was focused on the microchannel and afterwards a detection window of 50 µm x 50 µm (1:1 ratio) was chosen. Injection time of 25 seconds was selected. Signals (Peak area) were overloading in both cases so PMT Volts setting was switched from 900 V to 700 V. With a detection window adjusted to a size of 50 µm x 50 µm, average peak area of 6 consecutive runs of fluorescein was 3236,0 mV*s with a sd of 350,6 (RSD=10,8 %). On the other hand, when a detection window of 50 µm x 200 µm was used, average peak area of 6 consecutive runs of fluorescein was 7356,2 mV*s with a sd of 1105,7 (RSD=15,0 %). The detection window size of 50 µm x 50 µm was chosen for the following measurements on Zeiss microscope because of the two reasons. Firstly, even though the detection slit size of 50 µm x 200 µm gave much bigger signal (peak area) for the same concentration of fluorescein, the RSD was also bigger. That said, the results were less precise when larger detection window was used. Secondly, the signal was overloading when the larger detection window was applied (Figure 7). Considering that, the results weren't reliable because the detector reached its limit.
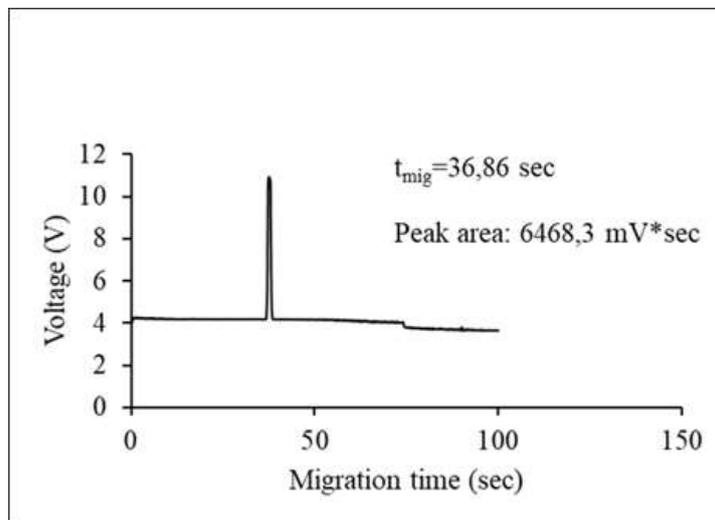
a)
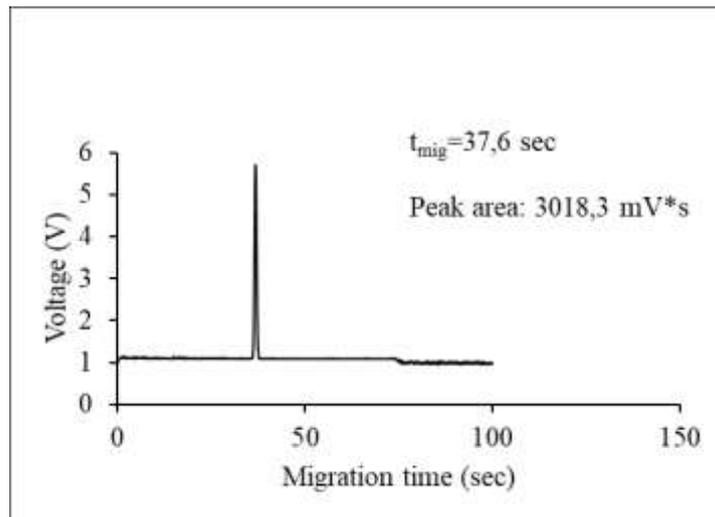
b)

Figure 7: MCE-LIF electropherogram of fluorescein (1 µM in 20 mM sodium borate buffer pH 10 at 500 Vcm^{-1}) in a allyl rich channel: a) test with a detection window size of 50 µm x 50 µm; b) test with a detection window size of 50 µm x 200 µm.

4.2. Optimization of Injection Time

For the purpose of choosing the best injection time, 1 µM fluorescein was used as sample and studied by MCE-LIF on allyl-rich thiol-ene microchip.

Table 3. Average migration time and peak area of 6 consecutive runs of fluorescein measured with different injection times.

	Injection time 15 s	Injection time 20 s	Injection time 25 s
Migration time ± sd [s]	40,38 ± 0,22	42,34 ± 0,50	40,02 ± 0,57
RSD (migration time)	0,54 %	1,19 %	1,42 %
Peak area ± sd [mV*s]	997,94 ± 115,35	1480,59 ± 70,28	2084,47 ± 302,42
RSD (peak area)	11,56 %	4,75 %	14,51 %

With the fluorescein sample three different tests were run with three different injection times: 15 s, 20 s and 25 s (Table 3). The largest peak area was accomplished by using injection time of 25 s. Accordingly, 25 s long injection time was chosen for the following measurements because the same concentration of fluorescein gave largest signal (peak area) with that time and by that many lower concentrations of fluorescein could be detected which would contribute to the sensitivity of the MCE-LIF method.

4.3. Optimization of Photomultiplier Tube Settings

The photomultiplier tube is an extremely sensitive light detector providing a current output proportional to light intensity. Photomultipliers are used to measure any process which directly or indirectly emits light. PMT is a photoemissive device in which the absorption of a photon results in the emission of an electron. These detectors work by amplifying the electrons generated by a photocathode exposed to a photon flux. Photomultipliers acquire

light through a glass or quartz window that covers a photosensitive surface, called a photocathode, which then releases electrons that are multiplied by electrodes known as metal channel dynodes. At the end of the dynode chain is an anode or collection electrode. Over a very large range, the current flowing from the anode to ground is directly proportional to the photoelectron flux generated by the photocathode. When the photomultiplier is operating, current flowing between the anode and ground (zero potential) is directly proportional to the photoelectron flux generated by the photocathode when it is exposed to incident photon radiation. The overall gain of the PMT is equal to the number of electrons produced at the anode for every photoelectron generated at the photocathode. As such, it is equivalent to the ratio of the anode current to the photocathode current. ("www.olympus-lifescience.com," n.d.).

Since both microscopes were connected with the same photomultiplier tube, all PMT settings were tested on Leica microscope. Only PMT gain setting was tested additionally while using Zeiss microscope. All the other settings were left the same as on Leica microscope except PMT gain. For each optimization of photomultiplier setting fluorescein was used as an analyte and was studied by MCE-LIF on allyl-rich thiol-ene microchannel. For offset and gain optimization the concentration of 1 µM fluorescein was used and for PMT volts the concentration of 100 nM fluorescein. Other PMT settings were left the same as in previous measurements. Comparison of different photomultiplier tube settings were primarily based on peak areas.

Table 4.: Average migration time and peak area of fluorescein measured with different PMT gain, offset and volts settings.

	PMT offset			PMT gain		PMT volts	
	off	*Low*	*High*	*Low*	*High*	*900 V*	*1000 V*
Migration time ± sd [s]	39,58 ±0,27	38,72 ±0,43	40,02 ±0,57	40,34 ±1,28	41,29 ±2,06	36,44 ±0,28	37,1 ±0,33
RSD (migration time)	0,69 %	1,10 %	1,42 %	3,17 %	4,98 %	0,77 %	0,90 %
Peak area ± sd [mV*s]	780,47 ±95,93	684,70 ±175,29	2084,47 ±302,42	11,91 ±9,59	901,13 ±105,77	266,01 ±64,83	215,96 ±76,87
RSD (peak area)	12,29%	25,60%	14,51%	80,53%	11,74%	24,37%	35,59%

PMT offset. Offset is an electronic adjustment that adds positive or negative voltage to the signal so that a selected background signal corresponds to a PMT output of ~0 volts. It should be adjusted so that the lowest signals are near the photomultiplier detection threshold. In practice, offset should be applied first before adjusting the photomultiplier gain. Offset changes the amplitude of the entire voltage signal, but since it is added to or subtracted from the total signal, it does not alter the voltage differential between the high and low voltage amplitudes in the original signal (Figure 8). For example, with a signal ranging from 4 to 18 volts that is modified with an offset setting of -4 volts, the resulting signal spans 0 to 14 volts, but the difference remains 14 volts (Douglas B. Murphy and Michael W. Davidson, 2012).
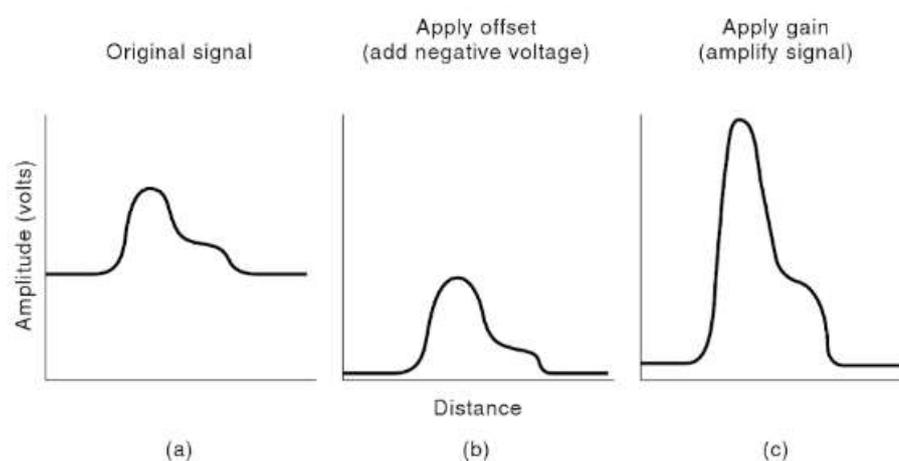

Figure 8. Gain and offset adjustment (Murphy and Davidson, 2012).

In this research, three different PMT offset settings were tested: off, low and high. For six consecutive runs of 1 µM fluorescein average migration time (in seconds) and peak area (mV*s) were calculated. Firstly, electropherograms (Figure 9) were examined visually. With HIGH setting selected background signal corresponded to a PMT output of ~4 volts. The OFF and LOW setting gave signals that were nearer the photomultiplier detection threshold. Furthermore, the OFF setting gave a signal with a peak area of 780,47 mV*s and a standard deviation of 95,93 (RSD=12,29%), (Table 4). When PMT offset was switched to LOW setting, peak area was 684,70 mV*s with a standard deviation of 175,29 (RSD=25,60%), (Table 4). OFF setting was chosen because it gave larger peak area then the LOW setting for the same concentration of fluorescein and by that many lower concentrations of fluorescein could be detected which would contribute to the sensitivity of the MCE-LIF method.
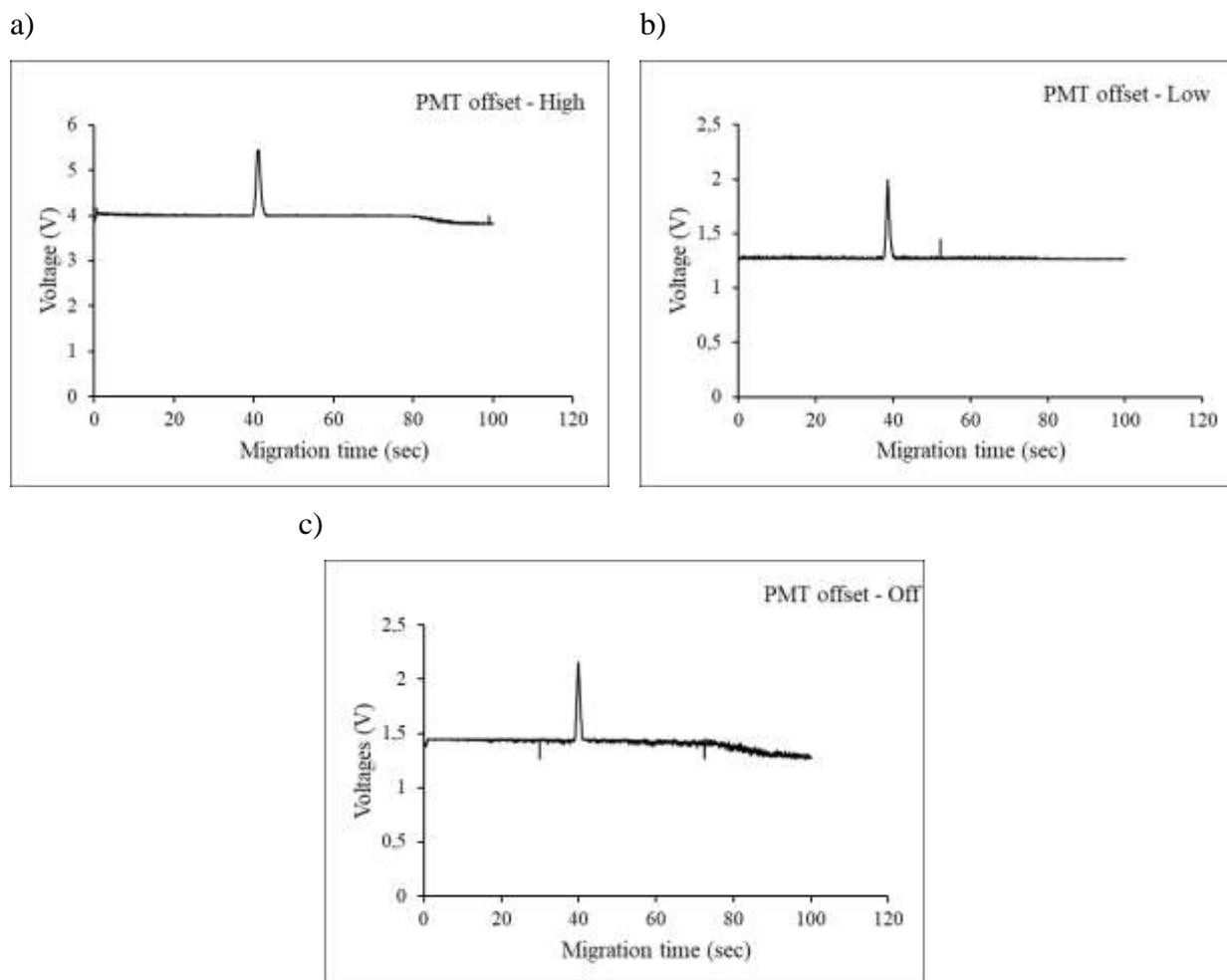
a)

b)

c)

Figure 9. Three MCE-LIF electropherograms of 1 µM fluorescein in an allyl rich channel. The MCE analysis was performed in 20 mM sodium borate buffer (pH 10,00) at 500 Vcm^{-1} with three different PMT offset settings: a) high, b) low, c) off.

PMT gain. The gain or current amplification of a photomultiplier tube is the ratio of the anode current to the photocathode current. One test was run for each setting (HIGH and LOW). For six consecutive runs of 1 µM fluorescein average migration time and peak area were calculated (Table 4). HIGH setting was chosen on PMT connected to Leica microscope because it gave larger peak area when same concentration of fluorescein was tested.

PMT Volts. For six consecutive runs of 100 nM fluorescein average migration time and peak area was calculated (Table 4) for each PMT volts setting (800 V, 900 V, 1000 V). When PMT volts setting of 800 V was applied signal wasn't detectable. PMT volts setting of 900 V gave a signal with a peak area of 266,01 mV*s (sd=64,38, RSD=24,37%). On the other hand, PMT

volts setting of 1000 V gave a signal with a peak area of 215,96 mV*s (sd=76,87, RSD=35,59%). The peak areas were very similar in both cases but the major difference between 900 V and 1000 V setting was that the baseline was much lower in the case of 900 V and that is why the voltage of 900 V was chosen for the following tests (Figure 10).
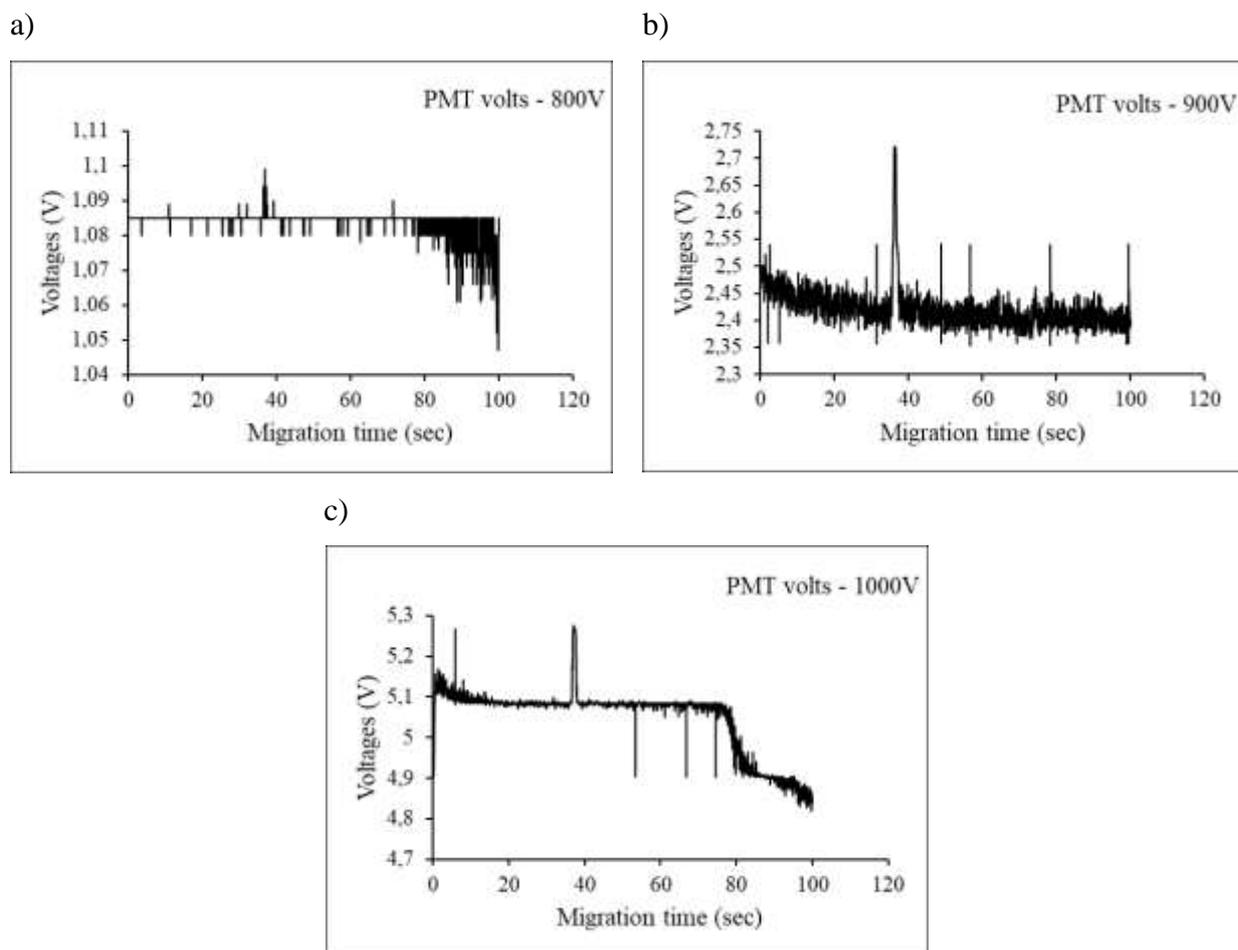
a)

b)

c)

Figure 10. Three MCE-LIF electropherograms of 100 nM fluorescein in an allyl rich channel. The MCE analysis was performed in 20 mM sodium borate buffer (pH 10,00) at 500 Vcm^{-1} with three different PMT volts settings: a) 800 V, b) 900 V, c) 1000 V.

PMT gain. PMT gain setting was additionally adjusted on photomultiplier tube connected to the Zeiss microscope. All other settings were left the same as on photomultiplier tube connected to Leica microscope. Four different PMT gain settings were tested: PMT gain 5,

PMT gain 6, PMT gain 7, PMT gain 8. For six consecutive runs of 1 µM fluorescein average migration time and peak area was calculated (Table 5).

Table 5: Average migration time and peak area of 1 µm fluorescein measured with different PMT gain setting.

	Photomultiplier gain setting			
	PMT gain 5	PMT gain 6	PMT gain 7	PMT gain 8
migration time (average ± sd) [s]	38,9 ± 2,4	39,5 ± 2,3	39,8 ± 2,4	40,4 ± 2,2
RSD (migration time)	6,1%	5,8%	5,9%	5,5%
peak area (average ± sd) [mV*s]	7495 ± 319	5230 ± 135	6619 ± 674	7794 ± 260
RSD (migration time)	4,3%	2,6%	10,2%	3,3%

The largest peak area of 7794 mV*s was achieved when PMT gain 8 was applied. The standard deviation of the peak area was 260 and this setting was chosen for the following measurements (Zeiss microscope).

4.4 Determination of Detection Limit and Quantitation Limit of Fluorescein

Detection (LOD) and quantitation limits (LOQ) represent method sensitivity. The detection limit (LOD) of an individual analytical procedure is the lowest amount of analyte in a sample, which can be detected but not necessarily quantitated as an exact value. Detection limit was determined from a calibration curve. The quantitation limit (LOQ) of an individual analytical procedure is the lowest amount of analyte in a sample, which can be quantitatively determined with suitable precision and accuracy. Quantitation limit was determined from a calibration curve. A specific calibration curve should be studied using samples, containing an analyte in the range of LOQ. Based on the standard deviation of the response and the slope the LOD and the LOQ were expressed as:

$$LOD = \frac{3,3 * \sigma}{S}$$

$$LOQ = \frac{10 * \sigma}{S}$$

where σ is the standard deviation of the response and S is the slope of the calibration curve. The estimate of σ was based on the calibration curve.

The samples containing analyte (fluorescein) in the range of LOD were studied by MCE-LIF on allyl-rich thiol-ene microchip. For each fluorescein concentration (1,25 nM, 2,5 nM, 5 nM, 10 nM, 20 nM, 40 nM) six consecutive injections were applied and average peak area and migration time were calculated for every sample concentration.
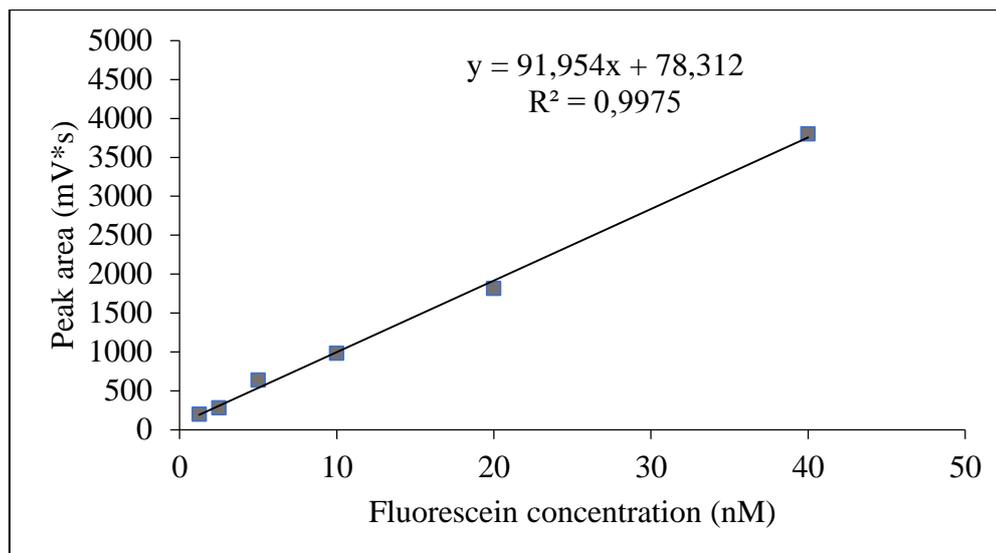
Figure 11. Fluorescein regression line over the range 1,25 nM – 40 nM.

The regression line over the range of 1,25 – 40 nM was y=91,954x + 78,312 with a coefficient of determination (R^2) of 0,9975. The LOD of fluorescein based on the calibration curve was 2,72 nM and the LOQ of fluorescein based on the calibration curve was 8,23 nM (Figure 11).

4.5 Analyses of Linearity by Fluorescein

The linearity of an analytical procedure is its ability (within a given range) to obtain test results which are directly proportional to the concentration (amount) of analyte in the sample. For the establishment of linearity, a minimum of 5 concentrations is recommended. Linearity was evaluated by visual inspection of a plot of signals (peak area in electropherogram) as a function of analyte (fluorescein) concentration. After that test results were evaluated by calculation of a regression line by the method of least squares. Simple linear regression models the relationship between a dependent variable and one independent variable using a linear function. The samples containing analyte (fluorescein) were studied by MCE-LIF on allyl-rich thiol-ene microchip. Stock of 5 mM fluorescein was diluted to following concentrations: 10 nM, 15 nM, 20 nM, 25 nM, 30 nM, 35 nM. For each fluorescein concentration six consecutive injections were applied and average peak area and migration time were calculated. For each concentration of fluorescein, the average peak area of the signal was calculated (Figure 12).
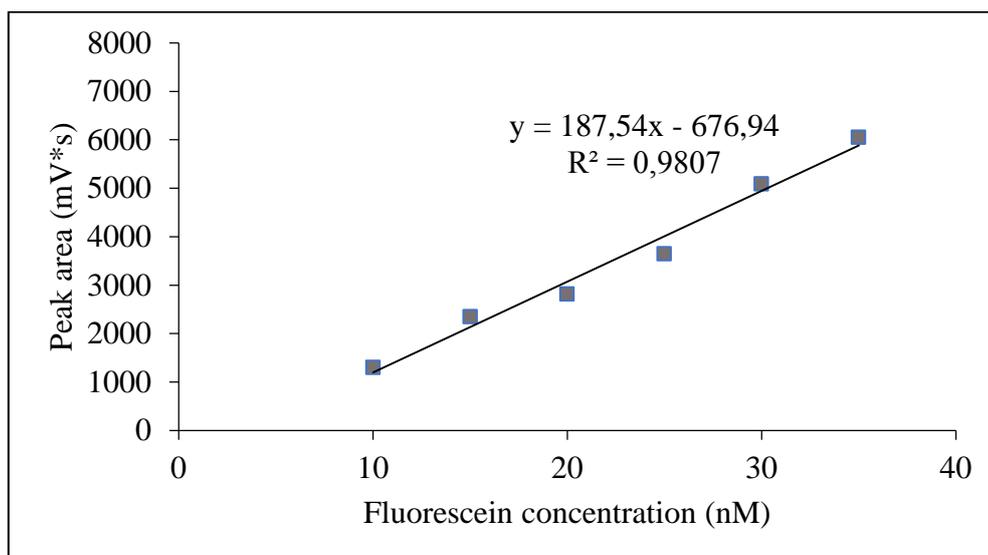
Figure 12. Fluorescein regression line over the range 10 – 35 nM.

A concentration range of 10 - 35 nM was visually determined to be the linear concentration range for fluorescein using MCE-LIF method. This range could further be explained by examining the regression line itself. The equation of the regression was y=187,54x-676,94 with a coefficient of determination (R^2) of 0,9807. R Square is used as an indicator of the goodness of fit. It shows how many points fall on the regression line. The R^2 value is calculated from the total sum of squares, more precisely, it is the sum of the squared deviations of the original data from the mean. In this study, the R^2 is 0,9807. It means that 98,07% of values fit the regression analysis model. In other words, 98,07% of the dependent variables (peak area) are explained by the independent variables (fluorescein concentrations). Multiple R is the Correlation Coefficient that can be any value between -1 and 1, and its absolute value indicates the relationship strength. The larger the absolute value, the stronger the relationship: 1 means a strong positive relationship, -1 means a strong negative relationship and 0 means no relationship at all. In this case Multiple R took value of 0,9903 which represents a strong positive relationship.

4.6 Detection Limit and Quantitation Limit of FITC SIINFEKL PEPTIDE (non interactive with virus)

Next, LOD and LOQ was determined for peptide FITC-SIINFEKL. Contrary to FITC-PolyK-SIINFEKL, FITC-SIINFEKL didn't include the positively charged 6K Lysine tail that was used for binding the PolyK-SIINFEKL to the virus. FITC-SIINFEKL was then used as an analogue model for determining the measuring concentrations. A calibration curve was made by measuring the signal-peak area (dependent variable) for samples containing a known concentration of analyte-FITC SIINFEKL peptide (independent variable). The tests were run on three different days. SIINFEKL peptide was studied by MCE-LIF on allyl-rich thiol-ene microchip. FITC SIINFEKL peptide stock off 1,25 µg/µL in H_2O was diluted (with 20 mM sodium phosphate buffer, pH 7,40) to obtain concentrations:

a) First day of measurements: 12,5 mg/L, 25 mg/L, 50 mg/L, 65 mg/L, 80 mg/L, 100 mg/L
b) Second day of measurements: 0,5 mg/L, 0,75 mg/L, 1 mg/L, 2,5 mg/L, 4 mg/L
c) Third day of measurements: 2,5 mg/L, 4 mg/L, 5 mg/L, 10 mg/L

For each FITC-SIINFEKL peptide solution several consecutive injections were applied and average peak area was calculated for each concentration (Figure 13).

The major problem that occurred while defining limit of detection and limit of quantitation of FITC-SINFEKL was repeatability. On first day higher concentrations of FITC-SIINFEKL peptide (12,5-100 mg/L) were tested then on other days. LOD and LOQ of FITC-SIINFEKL were 25,40 mg/L and 76,96 mg/L and both values were determined from a calibration curve. The problem occurred on the second day when same concentrations were tested again and the signal was overloading. Concentrations of FITC-SIINFEKL peptide were then lowered (0,5-4 mg/L) and new LOD and LOQ were calculated: 0,84 mg/L and 2,53 mg/L. On the third day while repeating same tests, first three concentrations of sample (0,5 mg/L, 0,75 mg/L, 1 mg/L) barely gave any signal. The conclusion was that the FITC-SIINFEKL was obviously adsorbing on the channel walls in capillary so surface modifications of the channel wall needed to be done to calculate right LOD and LOQ.
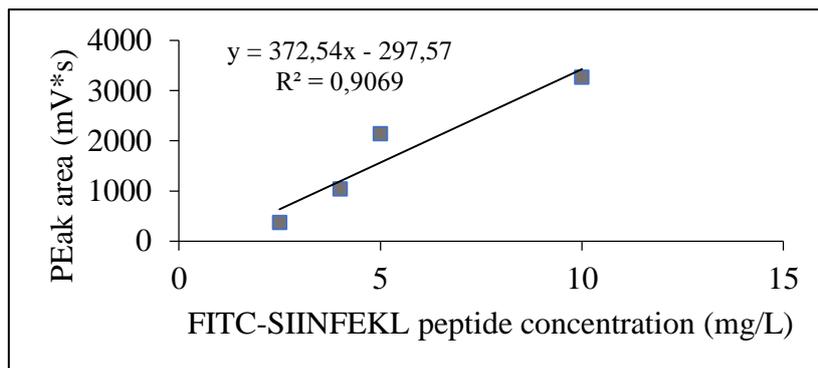
a)
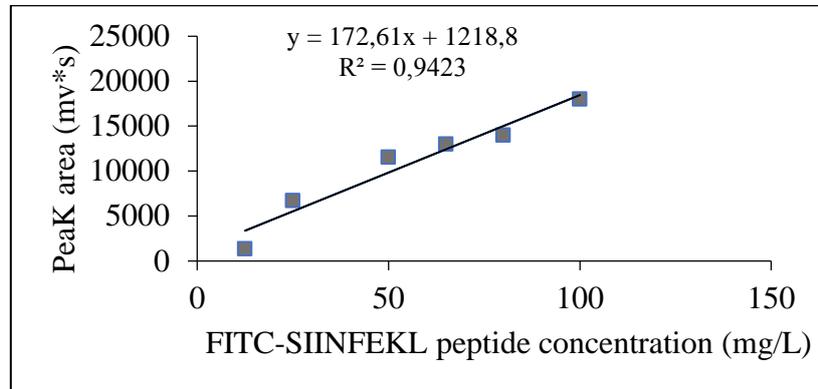
b)
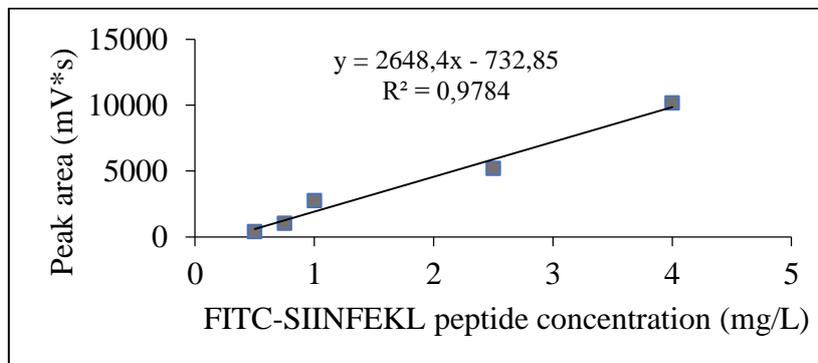
c)

Figure 13. FITC-SIINFEKL peptide regression lines over the range: a) 12,5-100 mg/L, b) 0,5-4 mg/L, c) 2,5-10 mg/L.

4.7 Surface Modifications of Thiol-ene Microchips

4.7.1 PEG Coating

Traditional covalent PEGylation (methoxy-PEG-thiol, MW 1000) was used as a surface treatment on allyl-rich thiol-ene microchips. Three different samples were tested on pegylated channels: 1 μm of Rhodamine 110 chloride, 25 mg/L of FITC-SIINFEKL peptide (non interactive with virus) and 50 mg/L of PolyK-SIINFEKL peptide (interactive with virus). Each sample was tested on different channels. For six consecutive runs of each sample, average migration time was calculated. The success of the coating of the channels was studied through the comparison of the migration times of Rhodamine 110 chloride. First, R_{110} was introduced into the native (non coated) channel and the average migration time was 30,35 s with a standard deviation of 0,39 and RSD of 1,30%. When the same sample of R_{110} was introduced into the coated channel, its average migration time was 49,1 s with a standard deviation of 1,96 and RSD of 3,98%. Since the coating of the channel prolonged the migration time of R_{110} and standard deviation and RSD values weren't significantly increased, the PEGylation of the channel was done successfully. Prolonged migration time of R_{110} indicated that the PEGylation of the allyl-rich thiol-ene channel decreased surface charge of the native allyl-rich surfaces.

Next, FITC-SIINFEKL peptide was introduced into the coated and non coated channels. Average migration time of the peptide in a native channel was 36,27 s with a standard deviation of 1,14 and RSD of 3,16%. When the same sample of FITC-SIINFEKL was introduced into the coated channel, its average migration time was 68,82 s with a standard deviation of 23,35 and RSD of 33,93%. Even though the migration time of the peptide was prolonged as expected since the surface charge of the allyl-rich surfaces decreased with PEGylation, standard deviation and RSD values were too high to consider the analysis precise. Despite successful coating, nonspecific interactions between the peptides and the microchannel could not be eliminated.

PolyK-SIINFEKL peptide unfortunately wasn't detectable so the adsorption of the protein on the channel wall was still present even after coating the capillary with PEG.

4.7.2 6k-peptide Coating

Since the PolyK-SIINFEKL peptide was still adsorbing onto the pegylated channels, dynamic coating of thiol rich thiol-ene microchips with the PolyK-SIINFEKL peptide analogue (non-fluorescent) was studied as an alternative approach. After filling the microchannels with peptide analogue, microchips were allowed to stand in the laminar flow hood for different amount of time to stabilize the coating. The peptide analogue coating was stabilized for 15 and 30 minutes. Two different samples were tested: Rhodamine 110 chloride and PolyK-SIINFEKL peptide (interactive with virus). Both analytes were tested on coated and non-coated microchannels. 300 nM solution of Rhodamine 110 chloride was tested and 10 and 20 mg/L solution of FITC-6k-peptide. For five consecutive runs of each sample (R_{110} and PolyK-SIINFEKL) average migration time was calculated.

Using the peptide analogue itself as the dynamic coating has showed more promising results then conventional PEGylation. The coating decreased significantly the migration time of Rhodamine 110 chloride in thiol-rich microchannels from 37,27 s in the native channels to 18,5 s and 19,29 s in the coated ones (Table 6). A decrease in the migration time of Rhodamine 110 chloride proved a successful coating. There wasn't major difference between 15 minutes and 30 minutes coating time except for the slightly lower standard deviation and RSD in the case of 30 minutes stabilization (Table 6). When 30 minutes coating was used standard deviation of the migration time was 0,50 and RSD was 2,61% which indicates that the data points (migration time) tend to be closer to the expected value and in the end more precise analysis was possible to achieve.

Table 6. Comparison of migration time of Rhodamine 110 chloride on peptide coated and non coated channel with 15 minutes stabilization time.

Analyte	Peptide coated channel		Native channel
Rhodamine 110 chloride (300 nM)	Duration of stabilization: 15 min	Duration of stabilization: 30 min	
Migration time [s]: -average -sd -RSD (%)	18,5 1,18 6,39	19,29 0,50 2,61	37,27 2,23 5,98

The dynamic peptide coating also facilitated MCE analysis of the fluorescent polyK-SIINFEK*L peptide. Matter of fact, FITC-6k-peptide wasn't detectable before peptide analogue coating of the microchannels. The comparison between analysis on native and coated microchannels in this case couldn't be done because FITC-6k-peptide didn't give any signals on the native microchannel since the beginning of the research. Only 15 minutes stabilization of coating was tested for the FITC-6k-peptide sample (Figure 14). 30 minutes coating in this case couldn't be tested because there were issues with the fabrication of the microchips in the end of the research. Five tests were made on the same microchannel with one sample injection in each. Average migration time for PolyK-SIINFEKL peptide was 88,74 s with a standard deviation of 23,33 and RSD of 26,29%. Standard deviation and RSD were very high and the peak area was significantly lower after each test. That said, probably the dynamic coating wasn't stabilized enough.
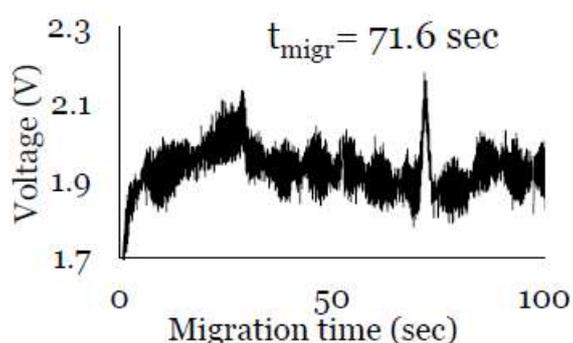

Figure 14. MCE-LIF electropherogram of the fluorescent polyK-SIINFEKL peptide (20 mg/L in 20 mM sodium phosphate buffer pH 7,4 at 500 Vcm^{-1}) in a thiol rich channel dynamically coated with the peptide analogue.

5 Conclusion

The aim of this thesis was to develop a MCE-LIF method for studying binding ratio of model MHC-I epitope peptide (PolyK-SIINFEKL peptide) to oncolytic CpG adenovirus (i.e. to find saturation point when the virus will be completely covered with the peptides). Microchip electrophoresis is a convenient tool for rapid determination of virus-peptide interactions, but it is challenged by strong nonspecific surface adsorption of the multiply charged peptide. Thiolene polymers, as the chosen chip material, provide increased flexibility in terms of specific, custom surface modifications.

For the optimization of the MCE-LIF method fluorescein and FITC-SIINFEKL peptide (non interactive with virus) were used as analytes. Settings adjustment such as detection slit size, injection time, photomultiplier tube settings and validation parameters such as detection limit, quantitation limit and linearity were demonstrated on fluorescein sample. Linearity reveals the relationship of signals (peak area) and analyte's concentrations (fluorescein). Linearity was evaluated by calculation of a regression line by the method of least squares. The equation of the regression was y=187,54x-676,94 with a coefficient of determination (R^2) of 0,9807. Multiple R took value of 0,9903 which represented a strong positive relationship. LOD and LOQ of fluorescein were determined from a calibration curve. The LOD based on the calibration curve was 2,72 nM and the LOQ based on the calibration curve was 8,23 nM. LOD, LOQ and linearity of FITC-SIINFEKL peptide wasn't determined because of its adsorption onto the microchannels.

Since the FITC-SIINFEKL peptide and PolyK-SIINFEKL peptide (interactive with virus) were adsorbing onto the microchannel surface the binding ratio between virus and peptide couldn't be studied in the end. For this reason, characterization of two different microchannel surface modification strategies were analyzed:

1) Traditional PEG coating on allyl-rich thiol-ene microchannels
2) Dynamic coating with a peptide analogue similar to the studied compound on thiol-rich thiol-ene microchannels.

Comparison between coated and non coated microchannels was done by comparing the migration times of Rhodamine 110 chloride on both types.

Conventional PEGylation was a viable approach to reduce both the surface charge and hydrophobicity of the native surfaces, as expected, but was not enough to eliminate nonspecific adsorption of the peptide on allyl-rich thiol-ene surfaces. PolyK-SIINFEKL peptide wasn't detectable on PEGylated microchannels.

Using the peptide analogue itself as the dynamic coating showed more promising results. The dynamic peptide coating facilitated MCE analysis of the fluorescent polyK-SIINFEKL peptide.

Future work concentrates on interaction studies between oncolytic adenoviruses and the tumor-specific PolyK-SIINFEKL peptide epitope.

6 References

Archambault JG, Brash JL. Protein repellent polyurethane-urea surfaces by chemical grafting of hydroxyl-terminated poly(ethylene oxide): effects of protein size and charge. *Colloids Surf. B Biointerfaces*, 2004, 33, 111–120.

Becker H, Gärtner C. Polymer microfabrication technologies for microfluidic systems. *Anal. Bioanal. Chem.*, 2008, 390, 89–111.

Belder D, Ludwig M. Surface modification in microchip electrophoresis. *Electrophoresis*, 2003, 24, 3595–3606.

Capasso C, Hirvinen M, Garofalo M, Romaniuk D, Kuryk L, Sarvela T, Vitale A, Antopolsky M, Magarkar A, Viitala T, Suutari T, Bunker A, Yliperttula M, Urtti A, Cerullo V. Oncolytic adenoviruses coated with MHC-I tumor epitopes increase the antitumor immunity and efficacy against melanoma. *Oncoimmunology*, 2016, 5.

Carlborg CF, Haraldsson T, Öberg K, Malkoch M, van der Wijngaart W. Beyond PDMS: off-stoichiometry thiol–ene (OSTE) based soft lithography for rapid prototyping of microfluidic devices. *Lab. Chip*, 2011, 11, 3136–3147.

Cramer NB, Bowman CN. Kinetics of thiol–ene and thiol–acrylate photopolymerizations with real-time fourier transform infrared. J. Polym. *Sci. Part Polym. Chem.*, 2001, 39, 3311–3319.

Cramer NB, Reddy SK, Cole M, Hoyle C, Bowman CN. Initiation and kinetics of thiol–ene photopolymerizations without photoinitiators. J. Polym. *Sci. Part Polym. Chem.*, 2004, 42, 5817–5826.

Cramer NB, Scott JP, Bowman CN. Photopolymerizations of Thiol−Ene Polymers without Photoinitiators. *Macromolecules*, 2002, 35, 5361–5365.

Culbertson CT, Ramsey RS, Ramsey JM. Electroosmotically Induced Hydraulic Pumping on Microchips: Differential Ion Transport. *Anal. Chem.*, 2000, 72, 2285–2291.

Cygan ZT, Cabral JT, Beers KL, Amis EJ. Microfluidic Platform for the Generation of Organic-Phase Microreactors. *Langmuir*, 2005, 21, 3629–3634.

Murphy DB, Davidson MW. Fundamentals of Light Microscopy and Electronic Imaging, 2nd Edition. USA, Wiley-Blackwell, 2012, pp. 221-222.

Efremova NV, Sheth SR, Leckband DE. Protein-Induced Changes in Poly(ethylene glycol) Brushes: Molecular Weight and Temperature Dependence. *Langmuir*, 2001, 17, 7628–7636.

Fasbender A, Zabner J, Chillón M, Moninger TO, Puga AP, Davidson BL, Welsh MJ. Complexes of Adenovirus with Polycationic Polymers and Cationic Lipids Increase the Efficiency of Gene Transfer in Vitro and in Vivo. *J. Biol. Chem.*, 1997, 272, 6479–6489.

Gomez-Sjoberg R, Leyrat A, Houseman BT, Shokat K, Quake SR. Biocompatibility and Reduced Drug Absorption of Sol-Gel-Treated Poly(dimethyl siloxane) for Microfluidic Cell Culture Applications. *Anal. Chem.*, 2010, 82, 21, 8954-8960.

Herr AE, Molho JI, Santiago JG, Mungal MG, Kenny TW, Garguilo MG. Electroosmotic Capillary Flow with Nonuniform Zeta Potential. *Anal. Chem.*, 2000, 72, 1053–1057.

Hoyle CE, Bowman CN. Thiol–Ene Click Chemistry. *Angew. Chem. Int. Ed.*, 2010, 49, 1540–1573.

Jacobson SC, Hergenroder R, Koutny LB, Ramsey JM. High-Speed Separations on a Microchip. *Anal. Chem.*, 1994, 66, 1114–1118.

Kingshott P, Wei J, Bagge-Ravn D, Gadegaard N, Gram L. Covalent Attachment of Poly(ethylene glycol) to Surfaces, Critical for Reducing Bacterial Adhesion. *Langmuir*, 2003, 19, 6912–6921.

Lu H, Stansbury JW, Bowman CN. Towards the elucidation of shrinkage stress development and relaxation in dental composites. *Dent. Mater.*, 2004, 20, 979–986.

Manz A, Graber N, Widmer HM. Miniaturized total chemical analysis systems: A novel concept for chemical sensing. Sens. *Actuators B Chem.*, 1990, 1, 244–248.

Manz A, Harrison DJ, Verpoorte EMJ, Fettinger JC, Paulus A, Lüdi H, Widmer HM. Planar chips technology for miniaturization and integration of separation techniques into monitoring systems: Capillary electrophoresis on a chip. *J. Chromatogr. A*, 1992, 593, 253–258.

McDonald JC, Whitesides GM. Poly(dimethylsiloxane) as a Material for Fabricating Microfluidic Devices. *Acc. Chem. Res.*, 2002, 35, 491–499.

Natali M, Begolo S, Carofiglio T, Mistura G. Rapid prototyping of multilayer thiolene microfluidic chips by photopolymerization and transfer lamination. *Lab. Chip*, 2008, 8, 492–494.

Ramsey JM, Jacobson SC, Knapp MR. Microfabricated chemical measurement systems. *Nat. Med.*, 1995, 1, 1093–1095.

Roach P, Farrar D, Perry CC. Interpretation of Protein Adsorption: Surface-Induced Conformational Changes. *J. Am. Chem. Soc.*, 2005, 127, 8168–8173.

Roosjen A, van der Mei HC, Busscher HJ, Norde W. Microbial Adhesion to Poly(ethylene oxide) Brushes: Influence of Polymer Chain Length and Temperature. *Langmuir*, 2004, 20, 10949–10955.

Sheth SR, Leckband D. Measurements of attractive forces between proteins and end-grafted poly(ethylene glycol) chains. *Proc. Natl. Acad. Sci.*, 1997, 94, 8399-8404.

Sikanen TM, Lafleur JP, Moilanen ME, Zhuang G, Jensen TG, Kutter JP. Fabrication and bonding of thiol-ene-based microfluidic devices. *J. Micromechanics Microengineering*, 2013, 23, 037002.

Tähkä SM, Bonabi A, Nordberg ME, Kanerva M, Jokinen VP, Sikanen TM. Thiol-ene microfluidic devices for microchip electrophoresis: Effects of curing conditions and monomer composition on surface properties. *J. Chromatogr. A*, 2015, 1426, 233–240.

Unsworth LD, Sheardown H, Brash JL. Protein Resistance of Surfaces Prepared by Sorption of End-Thiolated Poly(ethylene glycol) to Gold: Effect of Surface Chain Density. *Langmuir*, 2005, 21, 1036–1041.

Vickers JA, Caulum MM, Henry CS. Generation of Hydrophilic Poly(dimethylsiloxane) for High-Performance Microchip Electrophoresis. *Anal. Chem.*, 2006, 78, 7446–7452.

Volpatti LR, Yetisen AK. Commercialization of microfluidic devices. *Trends Biotechnol.*, 2014, 32, 347–350.

Wang D, Douma M, Swift B, Oleschuk RD, Horton JH. The adsorption of globular proteins onto a fluorinated PDMS surface. *J. Colloid Interface Sci.*, 2009, 331, 90–97.

Wei J, Ravn DB, Gram L, Kingshott P. Stainless steel modified with poly(ethylene glycol) can prevent protein adsorption but not bacterial adhesion. *Colloids Surf. B Biointerfaces*, 2003, 32, 275–291.

Concepts in Digital Imaging Technology - Photomultiplier Tubes, http://www.olympus-lifescience.com, accessed 7.12.19.

Zhang F, Kang ET, Neoh KG, Wang P, Tan KL, Surface modification of stainless steel by grafting of poly(ethylene glycol) for reduction in protein adsorption. *Biomaterials*, 2001, 22, 1541–1548.

Zheng J, Li L, Tsao HK, Sheng YJ, Chen S, Jiang S. Strong Repulsive Forces between Protein and Oligo (Ethylene Glycol) Self-Assembled Monolayers: A Molecular Simulation Study. *Biophys. J.*, 2005, 89, 158–166.

7 Summary

One of the limitations in protein analysis by microchip capillary electrophoresis (MCE) is the adsorption of the analytes onto the walls of the separation channel because of the electrostatic or hydrophobic interactions of proteins with the channel. Capillary coatings are required to prevent protein adsorption phenomena onto the capillary wall and to increase the repeatability of the separations. In addition of that, capillary coatings should thus ensure high separation efficiency and good repeatability.

In this work, thiol-ene based microchips were used for analysis of PolyK-SIINFEKL peptide. MCE-LIF(laser-induced fluorescence) method was developed in this work for future studying of binding ratios between oncolytic adenovirus and MHC-I epitope peptide (PolyK-SIINFEKL peptide). Since the peptides used in research have been fluorescently labeled with fluorescein isothiocyanate (FITC-peptides) optimization of the MCE-LIF method involved measurements of the fluorescein to adjust settings such as a detection slit size, injection time and photomultiplier tube settings. Validation characteristics such as detection limit, quantitation limit and linearity were demonstrated only on fluorescein samples due to the protein adsorption onto the microchannels (SIINFEKL peptide -non interactive with virus and PolyK-SIINFEKL peptide-interactive with virus). Successful microchannel coatings should have been done prior to method validation by FITC-peptides. Conventional PEGylation on allyl-rich thiol-ene microchannels was a viable approach to reduce both the surface charge and hydrophobicity of the native surfaces, as expected, but was not enough to eliminate nonspecific adsorption of the peptide on allyl-rich thiol-ene surfaces. Using the peptide non fluorescent analogue as the dynamic coating on thiol-rich thiol-ene microchannels showed more promising results. The dynamic peptide coating facilitated MCE analysis of the fluorescent polyK-SIINFEKL peptide on thiol-rich thiol-ene surfaces.

8 Sažetak

Jedno od najvećih ograničenja u analizi proteina kapilarnom elektroforezom na mikročipu je njihova adsoprcija na stijenku kapilare kao posljedica elektrostatskih i hidrofobnih interakcija. Prevlačenje kapilarnih stijenki nužno je kako bi se spriječila adsorpcija proteina i time povećala reproducibilnost separacije.

U ovom radu, korištene su tiol-en mikrokapilare za analizu PolyK-SIINFEKL peptida. Kapilarna elektroforeza na mikročipu s laser-induciranom fluorescencijom kao načinom detekcije (MCE-LIF), pokušala se razviti u svrhu proučavanja vezanja onkolitičkog CpG adenovirusa i MHC-I epitopa peptida (PolyK-SIINFEKL peptid) kako bi se našla točka zasićenja u kojoj bi virus bio kompletno prekriven PolyK-SIINFEKL peptidom. Budući da su peptidi korišteni u istraživanju obilježeni s fluorescein izotiocijanatom (FITC), fluorescein je korišten u svrhu optimizacije MCE-LIF metode odnosno podešavanja veličine detekcijskog prozora, vremena injektiranja i postavki fotomultiplikatora. Fluorescein je također korišten u svrhu validacije metode za određivanje linearnosti, granice detekcije i kvanitifikacije. Budući da su se FITC-peptidi korišteni u istraživanju adsorbirali na stijenku nemodificiranih kapilara, metoda se nije mogla validirati za prvobitnu primjenu te se istraživanje usredotočilo na prevlake kapilara putem kojih bi PolyK-SIINFEKL peptid i SIINFEKL peptid neometano stizali do detekcijskog prozora na kapilari. Unatoč tome što je kovalentna imobilizacija polietilen glikola na kapilarnim stijenkama očekivano snizila hidrofobnost stijenki kapilara, to nije bilo dovoljno da se eliminiraju nespecifične adsoprcije peptida na stijenci kapilare. Fizikalna adsoprcija peptidnog analoga PolyK-SIINFEKL peptida (nefluorescentnog) na kapilarnim stijenkama pokazala je obećavajuće rezultate. Ubrzala je MCE-LIF analizu PolyK-SIINFEKL peptida na tiol-en mikrokapilarama.

OPTIMIZATION OF MICROCHIP-BASED CAPILLARY ELECTROPHORESIS FOR STUDYING ONCOLYTIC ADENOVIRUS-PEPTIDE BINDING RATIO

Laura Batelić

SUMMARY

One of the limitations in protein analysis by microchip capillary electrophoresis (MCE) is the adsorption of the analytes onto the walls of the separation channel because of the electrostatic or hydrophobic interactions of proteins with the channel. Capillary coatings are required to prevent protein adsorption phenomena onto the capillary wall and to increase the repeatability of the separations. In addition of that, capillary coatings should thus ensure high separation efficiency and good repeatability.

In this work, thiol-ene based microchips were used for analysis of PolyK-SIINFEKL peptide. MCE-LIF(laser-induced fluorescence) method was developed in this work for future studying of binding ratios between oncolytic adenovirus and MHC-I epitope peptide (PolyK-SIINFEKL peptide). Since the peptides used in research have been fluorescently labeled with fluorescein isothiocyanate (FITC-peptides) optimization of the MCE-LIF method involved measurements of the fluorescein to adjust settings such as a detection slit size, injection time and photomultiplier tube settings. Validation characteristics such as detection limit, quantitation limit and linearity were demonstrated only on fluorescein samples due to the protein adsorption onto the microchannels (SIINFEKL peptide -non interactive with virus and PolyK-SIINFEKL peptide-interactive with virus). Successful microchannel coatings should have been done prior to method validation by FITC-peptides. Conventional PEGylation on allyl-rich thiol-ene microchannels was a viable approach to reduce both the surface charge and hydrophobicity of the native surfaces, as expected, but was not enough to eliminate nonspecific adsorption of the peptide on allyl-rich thiol-ene surfaces. Using the peptide non fluorescent analogue as the dynamic coating on thiol-rich thiol-ene microchannels showed more promising results. The dynamic peptide coating facilitated MCE analysis of the fluorescent polyK-SIINFEKL peptide on thiol-rich thiol-ene surfaces.

OPTIMIZACIJA METODE KAPILARNE ELEKTROFOREZE NA MIKROČIPU U SVRHU PRUČAVANJA VEZANJA ONKOLITIČKOG ADENOVIRUSA I PEPTIDA

Laura Batelić

SAŽETAK

Jedno od najvećih ograničenja u analizi proteina kapilarnom elektroforezom na mikročipu je njihova adsoprcija na stijenku kapilare kao posljedica elektrostatskih i hidrofobnih interakcija. Prevlačenje kapilarnih stijenki nužno je kako bi se spriječila adsorpcija proteina i time povećala reproducibilnost separacije.

U ovom radu, korištene su tiol-en mikrokapilare za analizu PolyK-SIINFEKL peptida. Kapilarna elektroforeza na mikročipu s laser-induciranom fluorescencijom kao načinom detekcije (MCE-LIF), pokušala se razviti u svrhu proučavanja vezanja onkolitičkog CpG adenovirusa i MHC-I epitopa peptida (PolyK-SIINFEKL peptid) kako bi se našla točka zasićenja u kojoj bi virus bio kompletno prekriven PolyK-SIINFEKL peptidom. Budući da su peptidi korišteni u istraživanju obilježeni s fluorescein izotiocijanatom (FITC), fluorescein je korišten u svrhu optimizacije MCE-LIF metode odnosno podešavanja veličine detekcijskog prozora, vremena injektiranja i postavki fotomultiplikatora. Fluorescein je također korišten u svrhu validacije metode za određivanje linearnosti, granice detekcije i kvanitifikacije. Budući da su se FITC-peptidi korišteni u istraživanju adsorbirali na stijenku nemodificiranih kapilara, metoda se nije mogla validirati za prvobitnu primjenu te se istraživanje usredotočilo na prevlake kapilara putem kojih bi PolyK-SIINFEKL peptid i SIINFEKL peptid neometano stizali do detekcijskog prozora na kapilari. Unatoč tome što je kovalentna imobilizacija polietilen glikola na kapilarnim stijenkama očekivano snizila hidrofobnost stijenki kapilara, to nije bilo dovoljno da se eliminiraju nespecifične adsoprcije peptida na stijenci kapilare. Fizikalna adsoprcija peptidnog analoga PolyK-SIINFEKL peptida (nefluorescentnog) na kapilarnim stijenkama pokazala je obećavajuće rezultate. Ubrzala je MCE-LIF analizu PolyK-SIINFEKL peptida na tiol-en mikrokapilarama.

Rad je pohranjen u Središnjoj knjižnici Sveučilišta u Zagrebu Farmaceutsko-biokemijskog fakulteta.